

See discussions, stats, and author profiles for this publication at: <https://www.researchgate.net/publication/273477753>

Diffractive optical elements to improve the quality of aberrated images

Article in *Journal of Optics* · April 2014

DOI: 10.1088/2040-8978/16/5/055706

CITATION

1

READS

105

3 authors:



Pedro J. Valle

Universidad de Cantabria

78 PUBLICATIONS 726 CITATIONS

[SEE PROFILE](#)



Miguel Ángel Cagigas García

Instituto de Astrofísica de Canarias

17 PUBLICATIONS 84 CITATIONS

[SEE PROFILE](#)



Manuel Cagigal

Universidad de Cantabria

134 PUBLICATIONS 1,039 CITATIONS

[SEE PROFILE](#)

Some of the authors of this publication are also working on these related projects:



Image superresolution [View project](#)



High contrast astronomical images [View project](#)

Diffraction optical elements to improve the quality of aberrated images

This content has been downloaded from IOPscience. Please scroll down to see the full text.

2014 J. Opt. 16 055706

(<http://iopscience.iop.org/2040-8986/16/5/055706>)

View [the table of contents for this issue](#), or go to the [journal homepage](#) for more

Download details:

IP Address: 193.144.183.154

This content was downloaded on 28/01/2015 at 16:51

Please note that [terms and conditions apply](#).

Diffractive optical elements to improve the quality of aberrated images

Pedro J Valle, Miguel A Cagigas and Manuel P Cagigal¹

Departamento de Física Aplicada, Universidad de Cantabria Avenida de los Castros 48, E-39005 Santander, Spain

E-mail: vallep@unican.es, mcagigasga@gmail.com and perezcm@unican.es

Received 25 November 2013, revised 20 February 2014

Accepted for publication 17 March 2014

Published 23 April 2014

Abstract

In this paper we introduce a simple diffractive optics technique to improve images distorted by propagating through an inhomogeneous medium. Diffractive elements are used to generate a series of slightly displaced overlapping replicas of the incoming wavefront which produces a local averaging of the field. We propose two different configurations depending on whether the field aberration is produced before or after (or in the pass through) the focussing or imaging optics. Furthermore, the aberration correction is achieved without the need of prior wavefront sensing or complex active compensating elements in contrast to adaptive optics (AO) and holographic techniques. Both numerical simulations and laboratory experiments show that the different kinds of proposed diffractive masks (DMs) (amplitude and phase) work efficiently in the two configurations. Since this technique is particularly suitable for compensating the highest spatial frequencies it seems to be appropriate to be combined with AO systems.

Keywords: diffractive optical elements, aberration compensation, adaptive optics

(Some figures may appear in colour only in the online journal)

1. Introduction

A light beam propagating through an inhomogeneous medium may suffer amplitude and phase alterations. However, non-absorbing media with not too strong refraction index fluctuations may only introduce phase distortions. This situation can be found in ground-based astronomy, free space laser communication, high power optical systems or high-resolution microscopy. A technique widely applied to compensate this distorting effect is adaptive optics (AO), where the shape of a deformable mirror is modified according to the information extracted from a wavefront sensor [1]. AO is currently producing good results, although the compensation of the highest spatial frequencies is still a technological challenge.

Moreover, several phase conjugating methods have also been used to correct aberrated wavefronts [2]. For example, the self-

pumped phase conjugation, based on the use of nonlinear photorefractive crystals [3, 4], or the phase conjugation using a holographic technique [2] based on an optically addressed liquid crystal [5, 6]. Recently, there have been interesting experiments using optical phase conjugation for compensating the aberrations introduced by a turbid media [7, 8].

A remarkable issue is the compensation of thermally induced wavefront aberrations in high power optical systems such as lithography machines, laser in material processing or gravitational wave detectors [9]. However, in most of these cases real-time feedback aberration control is not possible and classical techniques cannot be used.

In contrast to the mentioned techniques we propose the idea of aberration compensation as the result of coherent averaging. We introduce an analytical description showing that the compensation of slightly aberrated wavefronts can be carried out through the overlapping of a set of displaced wavefront replicas. The effect of superimposing displaced wavefronts is to produce a smoothed version of the original

¹ Author to whom any correspondence should be addressed.

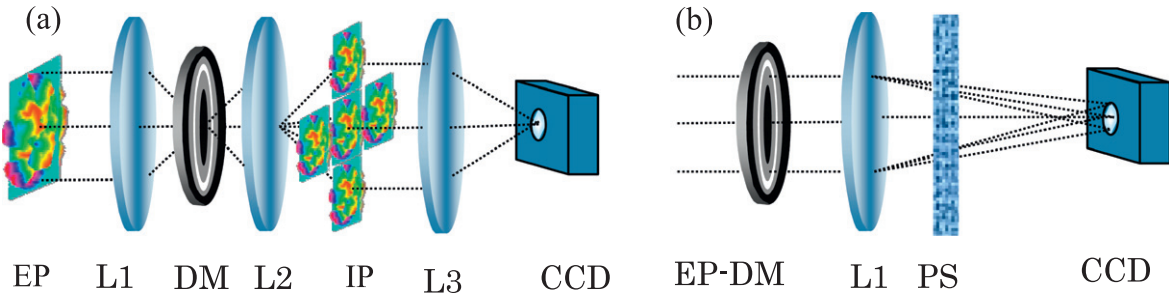


Figure 1. (a) DOES setup consisting on diffractive mask (DM) placed at the common focal plane of lenses L1 and L2. EP entrance pupil, IP intermediate pupil. Lens L3 forms the image onto the CCD. (b) DOES setup consisting on diffractive mask placed at the entrance pupil of lens L1 which forms an image onto the CCD after crossing an aberrating medium (phase screen, PS).

one. In previous papers [10, 11] we presented a simple method for designing diffractive optical elements by using Zernike polynomials. Now, we apply this method for designing diffractive optical devices for self-compensating aberrated wavefronts (DOES, diffractive optical elements for self-compensation). These devices produce the overlapping of a series of wavefront replicas, what achieves a local averaging of the incoming field. Since this averaging is performed over the field and not over the intensity, as in the commonly used enhancing image techniques, it allows increasing the contrast of the detected image keeping a high sharpness level. Moreover, the diffractive elements can also be disposed for compensation of distortions to be produced after (or meanwhile) passing through the optical system. In this case the averaging is achieved directly on the image plane.

The main advantages of DOES are that it can be carried out in a simple and controlled way and that it is a passive optical device in contrast to the active or AO systems. We have checked that compensation based on DOES is mainly effective averaging high order perturbations hence it seems that a proper combination of DOES and AO may be of great interest.

In this paper, we show how to design different kind of DMs that may produce a series of wavefront or image replicas distributed across the transversal plane or along the optical axis. The masks can be amplitude-only, phase-only and binary transmission. Numerical simulations are developed to check DMs performance in the two configurations. Simple laboratory experiments have also been carried out to verify the compensating effect of using the proposed devices.

2. DOES

The improvement of the image quality based on optical averaging has been known since many years. Commonly, the averaging of a set of images is performed in optical signal processing by means of a transmission mask consisting on an array of pinholes [12]. The use of this mask results in a large number of image replicas. When these replicas overlap, at least partially, the resulting image is a smoothed version of the original one.

We propose a new approach based on the similar idea of generating and averaging replicas but of a single aberrated wavefront as the system input. The mask will be a fully transmission able to produce only a reduced number of

overlapping replicas to avoid the energy to be addressed to useless replicas. Besides, the number, position and distance between replicas can be easily controlled by the mask design parameters.

In a previous work, we designed diffractive elements that, when placed at the pupil of an optical system, produced multiple foci [10]. The number and position of foci were directly governed by the diffractive element design parameters. This type of filters can be used to generate controlled replicas of incoming aberrated wavefronts. Figure 1(a) depicts a way to accomplish this. Lenses L1 and L2 form a standard 4f-system with a DM placed at the common focal plane. The first lens (L1) performs the Fourier transform of the input field, the transformed field is then multiplied by the transmission DM and Fourier transformed again by lens L2. Finally, an image is formed by lens L3 onto the detection system (CCD). As a result of introducing the mask, the entrance pupil field (EP) is multi-replicated at the intermediate pupil plane (IP). In this plane, original pupil averaging is achieved by adjusting the replica separations to overlap (not shown in figure 1(a) for clarity). From this smoother pupil wavefront an image less degraded than the original is expected on the final image plane.

2.1. DM profiles

A DM transmission profile providing four copies of the incoming wavefront, two of them displaced along the x -axis a magnitude proportional to $\pm\alpha$, and the other two along the y -axis a magnitude proportional to $\pm\alpha'$, can be obtained using a previously described procedure [11] (z -axis is assumed to be the optical axis and x - y plane the transversal plane),

$$M(x, y) = \cos(\alpha x) + \cos(\alpha' y). \quad (1)$$

Usually, we will take $\alpha' = \alpha$. A more efficient smoothing can be obtained using a higher number of replicas distributed along x , y and diagonal axes. These replicas can be easily obtained from the mask profile,

$$M(x, y) = \sum_{n,m} \left\{ \cos(\alpha_n x) + \cos(\alpha'_n y) + \cos[\beta_m(x+y)] + \cos[\beta'_m(x-y)] \right\}, \quad (2)$$

($n = 1$ to $N\alpha$, $m = 1$ to $N\beta$). The number and positions of the

pupil replicas are fixed through the mask parameters $N\alpha$, $N\beta$, α_n , α'_n , β_m and β'_m .

Other possible way for obtaining overlapping replicas is by the radially symmetric mask,

$$M(x, y) = \sum_m \cos[\alpha_m(x^2 + y^2)^{1/2}] = \sum_m \cos(\alpha_m r), \quad (3)$$

where r is the radial polar coordinate. To understand the average effect of using this mask we may evaluate the two-dimensional Fourier (one-dimensional Hankel) transform of circular cosine [13]:

$$\begin{aligned} m(\rho) &= FT[\cos(\alpha r)] \\ &= \frac{\alpha}{(2\pi)^2} \left[\left(\frac{\alpha}{2\pi} \right)^2 - \rho^2 \right]^{-3/2} \text{rect}\left(\frac{\pi\rho}{\alpha}\right), \end{aligned} \quad (4)$$

where $\text{rect}(\pi\rho/\alpha)$ means truncation to zero beyond the circle of radius α/π . Equation (4) represents a function with an impulsive ring shape behaviour. Hence, when in the L1 focal plane (see figure 1(a)) the Fourier transform of any aberrated wavefront is multiplied by the mask given in (3), the convolution product of the wavefront with the ring-like function given by (4) is obtained in the IP plane. This convolution provides a smoothed version of the original aberrated wavefront. In general, it is enough to take $m = 1$ to get good results.

We also propose to distribute pupil replicas not only across the x - y plane but along the z -axis. To get m couples of pupil replicas placed before and after the IP plane (figure 1(a)) we used the mask [10],

$$M(x, y) = \sum_m \cos[\alpha_m(x^2 + y^2)] = \sum_m \cos(\alpha_m r^2). \quad (5)$$

The number of replicas and their distances to the IP plane can be set through the design parameters m and α_m , respectively. In this case, on the IP plane a smoothed wavefront is obtained by superposition of the slightly defocused pupil copies.

Since the DMs are placed at an intermediate image plane, the zero transmittance areas of the amplitude-only masks make some parts of the object to be lost. In addition, fabrication of transmittance continuous DM may be difficult and expensive. Hence, the use of phase-only masks may be of great practical interest. It is possible to obtain a phase only mask from (2, 3 and 5) using the conversion,

$$PM(x, y) = \exp[iM(x, y)]. \quad (6)$$

Also binary versions of masks given by (2, 3 and 5) can be obtained with only applying a threshold. The binary mask $BM(x, y)$ will take zero value in all points except in those where the $M(x, y)$ values are above the threshold. Then, binary phase masks can be obtained introducing $BM(x, y)$ instead of $M(x, y)$ in (6). Phase and binary phase masks produce as good results as the corresponding amplitude-only ones, as we will see later.

3. Theory and numerical simulation

The mathematical treatment of the wave propagation was within the scalar diffraction theory and the Fourier optics approach. Computer simulations using the Matlab fast Fourier transform routine were carried out. To achieve a good spatial sampling and to avoid aliasing effects, 1024×1024 data samples were used. The system pupil was simulated with a 128×128 data sampling.

The incoming aberrated field at the system EP can be expressed as $E(x, y) = A \exp(i\phi(x, y))$, where A is the constant amplitude and $\phi(x, y)$ is the wavefront aberration function. In order to simulate general aberrating media we make use of the numerical method employed for atmospheric aberration simulations. Series of aberrated wavefronts (or aberrating phase screens (PS)) $\phi(x, y)$ were calculated according to [14] for a number of atmospheric conditions as it was shown in [15]. Atmospheric condition (i.e. amount of aberration) is determined by the ratio D/r_0 , where D is the telescope diameter and r_0 the atmospheric Fried parameter. We consider aberrations from $D/r_0 = 0$ (unaberrated) to $D/r_0 = 9$ (highly aberrated). High aberration is assumed when the halo peak intensity contributes more to the Strehl ratio than the coherent peak intensity, that is for $D/r_0 > 7.8$ [1].

4. Aberration compensation

As we mentioned in the introduction, we consider two practical situations corresponding to the cases where the propagation through an inhomogeneous medium occurs before or after (also meanwhile) passing through the imaging or focusing system. Both situation are illustrated in figures 1(a) and (b). The first case is referred to as postcorrection of previously distorted wavefronts and the second one as prior compensation of later aberrated wavefronts.

4.1. Previously aberrated wavefronts

When a wavefront which has been previously distorted as a result of its propagation through an inhomogeneous medium is focused by an optical system, we obtain a degraded image. To partially recover the image quality we propose the use of the DOES arrangement sketched in figure 1(a).

Considering, for example, a mask of the type described by (2) and assuming low aberration, the field at IP plane (lens L2 focal plane) will consist on a series of overlapping copies of the incoming field slightly displaced. This field can be mathematically expressed by

$$\begin{aligned} E_{IP}(x, y) &\approx \frac{1}{N} \sum_{n,m} E(x + \Delta x_n, y + \Delta y_m) \\ &\approx A \exp \left[i \frac{1}{N} \sum_{n,m} \phi(x + \Delta x_n, y + \Delta y_m) \right]. \end{aligned} \quad (7)$$

The total number of copies N is set by $N\alpha$ and $N\beta$, and Δx_n and Δy_m are the displacements related to α and β in (2).

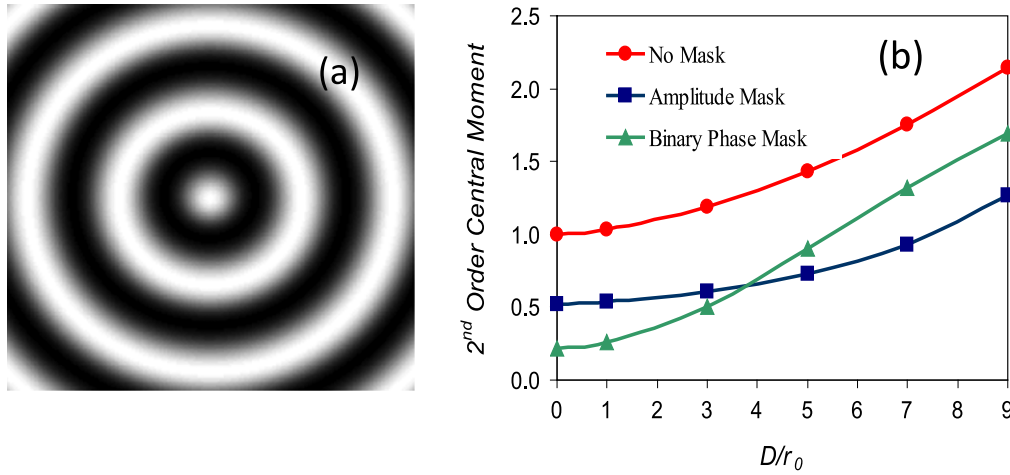


Figure 2. (a) Diffractive mask transmittance function corresponding to (3) with $m = 1$. (b) Averaged PSF second-order central moment as a function of the aberration degree. Moment value for unaberrated PSF has been set to unity.

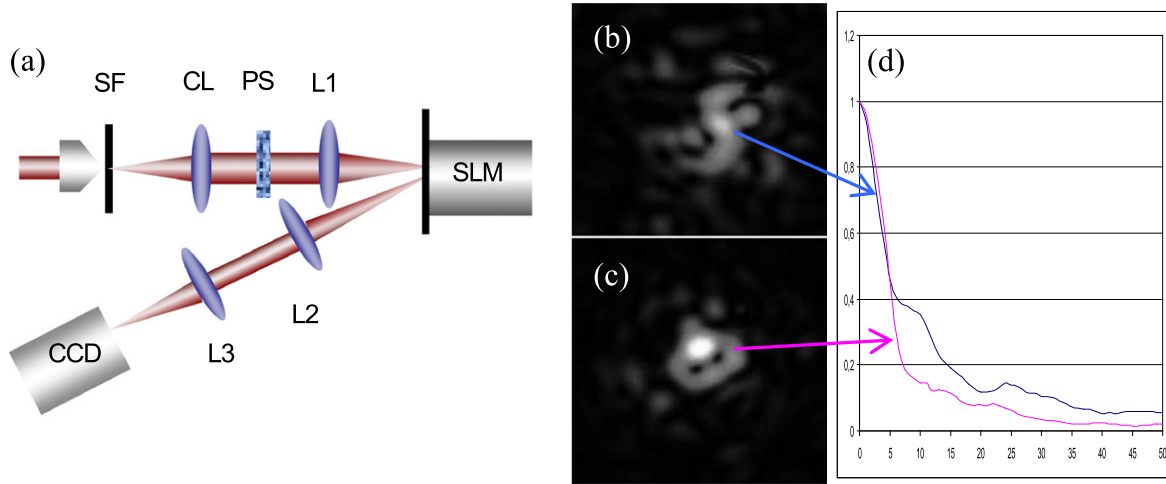


Figure 3. (a) Experimental setup: the distorting phase screen PS is introduced before focusing. (b) Aberrated PSF on the CCD without compensation. (c) Averaged PSF when the SLM reproduces the DM of (2). (d) Comparison of the normalized radial averaged energy in (b) and (c).

Hence, it can be seen in (7) that averaging slightly aberrated fields is equivalent to locally average the wavefront.

To quantify the image quality improvement produced by the DOES, we have evaluated the second-order central moment of the light intensity distribution at the image plane due to an incident plane wave passing through an aberrating medium. The second-order central moment measures the spread out of the aberrated point spread function (PSF) and it is considered an optical quality metric. The evaluation has been carried out by computer simulation for 100 PS realizations and the process has been repeated for a range of aberration degrees (a series of the D/r_0 values). As an example of the aberrated PSF second-order moments, figure 2 shows the case of the radially symmetric amplitude-only DM given by (3) for $m = 1$ and its binary phase version by (6). A clear reduction of the PSF second-order value appears as a consequence of using the DOES for a wide range of aberrations. It can be seen that binary phase masks are more efficient for low aberrated wavefronts than amplitude masks, but this

advantage disappears when the amplitude of the phase perturbation increases.

An experimental test has also been carried out with the setup shown in figure 3(a). The light source consists on a He-Ne laser (633 nm) which is spatially filtered and collimated using the lens CL (focal length: 60 cm). The plane wavefront so obtained is distorted by a PS introduced in the pathway. Lens L1 focuses the light onto a Hamamatsu spatial light modulator (SLM) (model PPM X8267) that can work in amplitude-only or phase-only modes. The light reflected on the modulator surface is collimated by the lens L2 (focal length: 40 cm) being focused by lens L3 (focal length: 40 cm) onto the CCD camera (model uEye 1540C).

When the SLM is not active (flat modulation) the lens L3 forms on the CCD a distorted PSF, figure 3(b). When the profile given by (2), with $n = m = 1$, $\alpha' = \alpha$ and $\beta' = \beta$, is introduced into the SLM, the aberrated PSF is partially corrected, as it can be seen by the bright spot in the centre of figure 3(c). The calculated value of the light intensity

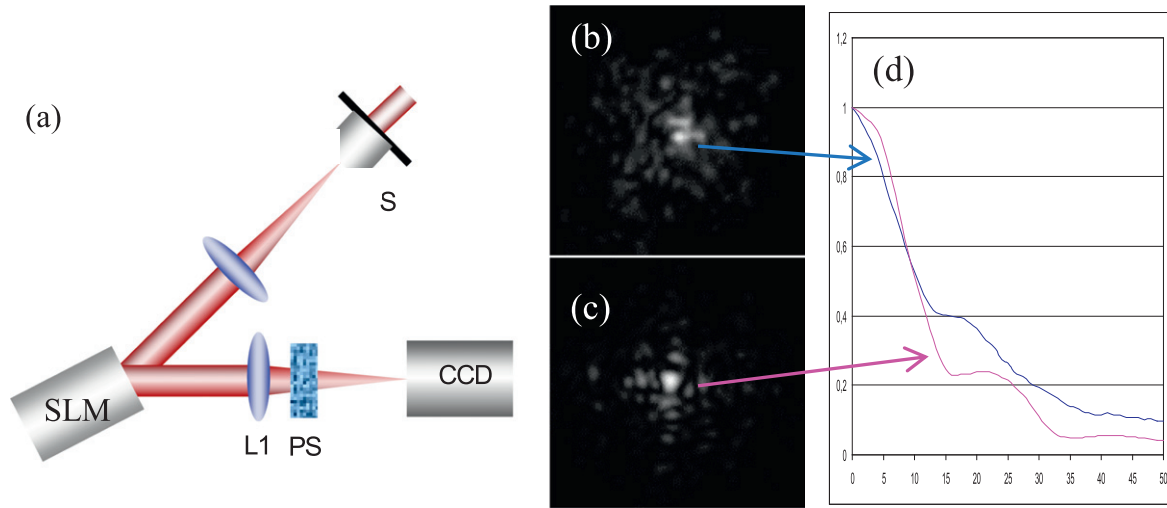


Figure 4. (a) Experimental setup: the distorting phase screen is introduced after lens L1. (b) Aberrated PSF without DOES. (c) Averaged PSF using an amplitude-only DOES. (d) Normalized radial averaged energy in (b) and (c).

second-order central moment for figure 3(c) is about 10% lower than that for figure 3(b). The normalized radial averaged energy of figures 3(b) and (c) is shown in figure 3(d) and shows that the PSF sharpness has been clearly improved.

Although the amplitude-only profiles provided excellent results, they also produce unwanted amplitude modulation on the image intensity distribution. To avoid this amplitude modulation we have also checked phase-only DM obtained according to (6) for the three kinds of masks shown in (2), (3) and (5). All of them perform satisfactorily, although the most energy efficient are the masks derived from (3).

The DOES compensation of previously aberrated wavefronts has different fields of application as for example where a light beam degraded by the atmosphere needs to be corrected before detection. That is the case of ground-based astronomy and free-space laser communication [16].

4.2. Post aberrated wavefronts

Another field of application is the reduction of the distorting effects appearing in the PSF due to the beam propagation through an aberrating medium placed after the optical system (or through the optical system itself), as sketched in figure 1(b).

Let us consider an incident plane wave (amplitude A) and the system EP described by the function $W(x, y)$. Let $PS(x, y) = \exp[i(\phi(x, y))]$ be the PS modelling the propagation through the aberrating medium (the optical system itself or an inhomogeneous medium placed at short distance from it). The aberrated image field, E_{ab} , can be obtained from the Fourier transform,

$$\begin{aligned} E_{ab}(u, v) &= FT[AW(x, y)PS(x, y)] \\ &= Aw(u, v) * ps(u, v), \end{aligned} \quad (8)$$

where $*$ stands for convolution product, $w(u, v)$ corresponds to the unaberrated image and $ps(u, v)$ to the Fourier transform of the PS (u, v are proportional to image plane coordinates). When introducing a DOES on the EP plane, for example of

the type described by (2), the modified image field can be expressed as,

$$\begin{aligned} E_{DOES}(u, v) &= Aw(u, v) * \frac{1}{N} \sum_{n,m} ps(u + \Delta u_n, v + \Delta v_m) \\ &= \frac{1}{N} \sum_{n,m} E_{ab}(u + \Delta u_n, v + \Delta v_m). \end{aligned} \quad (9)$$

From (9) it can be seen that a number of the original aberrated PSF will be obtained at different detector places. In general, every image will be slightly different since field must cross different parts of the aberrating medium before reaching the detector. When the distance between images is small a kind of image averaging is produced as a result of the superposition of the different aberrated PSF. It is interesting to note that in contrast to section 4.1, now the average occurs at the image plane.

This DOES configuration has been experimentally tested with the set-up shown in figure 4(a). A collimated beam is amplitude or phase modulated using the SLM. The lens L1 focuses the beam through an aberrating PS towards the CCD.

After checking all the DM sets we have seen that the best performing are those given by (2). Figure 4(b) shows the aberrated PSF of the optical system (lens L1) after placing a particular PS and figure 4(c) shows the same case after using a DOES. The calculated value of the light intensity second-order central moment for figure 4(c) is about 15% lower than that for figure 4(b). Figure 4(d) shows the comparison of their corresponding normalized radial averaged energy. It can be seen that, as a result of using the DOES, the energy is more symmetrically distributed and tends to be concentrated at the PSF centre.

The DOES compensation of wavefronts that will be aberrated later can be applied to the problem of thermally induced aberration in high power optical systems [9], focusing through a thick aberrating medium [17] and to the correction of specimen-induced aberrations in high-resolution optical microscopy [18].

5. Conclusions

We have proved that the use of a diffractive element may partially correct or compensate aberrated wavefronts. This is a kind of passive self-compensation that does not need wavefront sensing or deformable mirrors to operate and it is named as DOES, diffractive optical elements for self-compensation.

In the case of a previously aberrated wavefront, the compensation can be understood in terms of the averaging of the incoming wavefront produced by the coherent overlapping of a number of wavefront replicas. In the case of aberration occurring meanwhile or after passing the optical system, the average is the result of the overlapping of displaced PSF so that every PSF replica is affected by slightly different aberrations. In both cases the replicas, generated by the diffractive element, can be distributed in the x - y plane or along the z -axis. The field averaging, unlike intensity averaging, allows an image contrast increase by maintaining a high sharpness level.

We have checked by numerical simulation that both amplitude-only and phase-only DOES provide a significant improvement of the optical image quality. Nevertheless, phase-only masks seem to be more appropriate since they are more energy efficient. These conclusions have also been confirmed by mean of simple laboratory experiments.

Since the self-compensation provided by DOES can be interpreted in terms of the smoothing of the wavefront highest frequencies, the combination of DOES with low order AO devices may be particularly useful to achieve a high compensation level in an easy way.

Finally, let's remark that there are a number of fields where this partial compensation may be fruitfully applied like specimen induced aberrations in high resolution microscopy, thermally induced aberrations in high power optical systems or atmospheric aberration in free-space communications and ground-based astronomy.

Acknowledgements

This research was supported by the Ministerio de Economía y Competitividad under project FIS2012-31079.

References

- [1] Hardy J W 1998 *Adaptive Optics for Astronomical Telescopes* (Oxford: Oxford University Press)
- [2] Goodman J W 1996 *Introduction to Fourier Optics* (New York: McGraw-Hill)
- [3] Feinberg J 1982 Self-pumped, continuous-wave phase conjugator using internal-reflection *Opt. Lett.* **7** 486–8
- [4] Woerdemann M, Alpmann C and Denz C 2009 Self-pumped phase conjugation of light beams carrying orbital angular momentum *Opt. Express* **17** 22791–9
- [5] Mao C C, Johnson K M and Moddel G 1991 Optical phase conjugation using optically addressed liquid crystal light modulators *Opt. Lett.* **15** 1114–6
- [6] Johnson K M, Mao C C, Moddel G, Handschy M A and Arnett K 1990 High-speed low-power optical phase conjugation using a hybrid amorphous silicon/ferroelectric-liquid-crystal device *Opt. Lett.* **15** 1114–6
- [7] Tseng S H and Yang C 2007 2-D PSTD simulation of optical phase conjugation for turbidity suppression *Opt. Express* **15** 16005–16
- [8] Thakur A and Berakdar J 2012 Reflection and transmission of twisted light at phase conjugating interfaces *Opt. Express* **20** 1301–7
- [9] Harber A, Polo A, Maj I, Pereira S F, Urbach H P and Verhaegen M 2013 Predictive control of thermally induced wavefront aberrations *Opt. Express* **21** 21530–41
- [10] Valle P J and Cagigal M P 2012 Analytic design of multiple-axis, multifocal diffractive lenses *Opt. Lett.* **37** 1121–3
- [11] Cagigal M P and Valle P J 2012 Wavefront sensing using diffractive elements *Opt. Lett.* **37** 3813–5
- [12] Iizuka K 2008 *Engineering Optics* (Berlin: Springer)
- [13] Amidror I 1997 Fourier spectrum of radially periodic images *J. Opt. Soc. Am. A* **14** 816–26
- [14] Roddier N 1990 Atmospheric wavefront simulation using Zernike polynomials *Opt. Eng.* **29** 1174–80
- [15] Cagigal M P and Canales V F 1998 Speckle statistics in partially corrected wave fronts *Opt. Lett.* **23** 1072–4
- [16] Weyrauch T and Vorontsov M A 2004 Free-space laser communications with adaptive optics: atmospheric compensation experiments *J. Opt. Fiber Commun. Rep.* **1** 355–79
- [17] Stockbridge C, Lu Y, Moore J, Hoffman S, Paxman R, Toussaint K and Bifano T 2012 Focusing through dynamic scattering media *Opt. Express* **20** 15086–92
- [18] Simmonds R D and Booth M J 2013 Modelling of multi-conjugate adaptive optics for spatially variant aberrations in microscopy *J. Opt.* **15** 94010–8